P1.6 SIMULATED IMPACTS OF ENHANCED CCN AND GIANT-CCN CONCENTRATIONS ON OROGRAPHIC SNOWFALL

Stephen M. Saleeby[1]*, William Cotton[1], Douglas Lowenthal[2], Randolph Borys[2], Melanie Wetzel[2], Ian McCubbin[2], Michael Meyers[3]

[1]*Department of Atmospheric Science, Colorado State University, Fort Collins, CO*
[2]*Desert Research Institute, Reno, NV*
[3]*National Weather Service, Grand Junction, CO*

1. INTRODUCTION

The Park Range of Colorado receives the majority of its annual precipitation in the form of snow during the winter months. This north/south oriented mountain range is generally aligned orthogonally to the westerly mean flow that accompanies most synoptic mid-latitude cyclones over the western U.S. (see Fig. 1). In the absence of blocked flow, deep lifting of a near-surface airmass from the west can be transported over the crest of the Park Range. This deep lifting along the slope provides for enhanced condensate production and surface snowfall. The strong cross-barrier pressure gradient and upslope wind also tend to produce an orographic cloud with supercooled liquid water (Rauber et al., 1986; Borys et al., 2000). These supercooled cloud events are often observed during the winter months at the Desert Research Institute's Storm Peak Lab (SPL). SPL is a high-altitude research facility located atop Mt. Werner (~3210m MSL) near Steamboat Springs, CO (Borys and Wetzel, 1997).

A seeder-feeder mechanism, involving the sedimentation of higher altitude snow crystals through the low-level orographic cloud, produces greater precipitation amounts near mountaintop due to ample riming of cloud droplets in the lowest 2 km (Rauber et al., 1986). This low-level riming process enhances the precipitation efficiency, such that, the amount of rime has been shown to comprise from 20-50% of the final snow mass that reaches the surface (Borys et al., 2003). Enhanced riming will increase the mass of snow crystals as well as the fall speed; this increases the likelihood of higher snow deposits along windward slopes (Hindman, 1986). Slower falling, unrimed snow crystals are more likely to fall on the leeward slopes where subsidence leads to evaporation and disappearance of the "feeder" cloud.

While topography and riming may result in locally enhanced snowfall, intrusions of high concentrations of pollution aerosols can modify the condensate fields. Additions of sulfate-based cloud condensation nuclei (CCN) and giant-CCN (GCCN) can modify the liquid droplet spectra in the supercooled orographic feeder cloud. Changes in the size distributions will impact the snow riming efficiency. This study examines the relative impacts of CCN and GCCN number concentrations on total snowfall distributions near the Park Range of Colorado. This is accomplished using a mesoscale model to produce high resolution simulations of orographic snowfall events.

Corresponding author address: Stephen M. Saleeby, Colorado State Univ., Atmos. Sci. Dept., Fort Collins, CO 80523; e-mail: smsaleeb@atmos.colostate.edu

2. MODEL DESCRIPTION

The Colorado State University - Regional Atmospheric Modeling System (RAMS) Version 4.3 has been utilized for a set of sensitivity simulations with varying amounts of CCN and GCCN number concentration. The non-hydrostatic, compressible version of RAMS is configured on an Arakawa-C grid and sigma-z terrain-following coordinate system (Cotton et al., 2003). For these simulations, the model uses a nested 4-grid arrangement centered over Colorado. The outer grid-1 covers the continental United States with 60km grid spacing, grid-2 covers Colorado and the adjacent surrounding states with 15km grid spacing, grid-3 encompasses much of Colorado with 3km grid spacing, and grid-4 covers the north-south oriented Park Range from the cities of Hayden to Walden with 750m grid spacing (Fig. 1). Within each grid there are 40 vertical levels with a minimum of 75m grid spacing. The model uses vertical grid stretching with a stretch ratio of 1.12 and a maximum vertical grid spacing of 750m.

The RAMS model contains a microphysics package that predicts two-moments of the hydrometeor distributions (mixing ratio and number concentration) for rain, pristine ice, snow, aggregates, graupel, and hail (Meyers et al. 1997). Saleeby and Cotton (2004) extended the two-moment approach to the cloud droplet distribution via a parameterization for the formation of cloud droplets from activation of CCN and/or GCCN within a lifted parcel. A Lagrangian parcel model of was used to determine the percent of user-specified nuclei that would activate and grow by condensation into cloud droplets for a given ambient temperature, vertical velocity, and median radius of the aerosol distribution. Saleeby and Cotton (2008) introduced a binned approach to riming within the bulk microphysics framework in which realistic collection efficiencies are used to compute the collision-coalescence between ice crystals and cloud droplets. The hydrometeor distributions are decomposed into 36 size bins for riming computations of all possible size interactions. This method is much improved over the bulk riming method which applied a single collection efficiency value to the full size distribution. The CCN and GCCN concentrations (N_{CCN} and N_{GCCN}, respectively) were initialized horizontally homogeneous with a vertical profile that decreases linearly with height up to 4km

AGL. Initial surface N_{CCN} were specified at 100 and 1900 cm^{-3} and N_{GCCN} of 0.00001 and 0.5 cm^{-3}. The lower value is meant to represent clean conditions and the upper value, polluted conditions. The minimum concentration allowed at any location was 100 cm^{-3} for CCN and 0.00001 cm^{-3} for GCCN. The aerosol concentrations are represented on a poly-disperse lognormal distribution with a median radius for CCN of 0.04μm and GCCN of 3.0μm. As a source/sink function, CCN and GCCN are depleted upon droplet nucleation and replenished upon droplet evaporation. Simulations were conducted for a heavy riming, heavy snowfall event from February 11-13, 2007. The North American Regional Reanalysis was used for model initialization.

3. MODEL RESULTS AND OBSERVATIONS

Simulations of this snowfall event over the Park Range performed rather well with regards to snowfall amounts and the presence of a supercooled liquid water cloud with high liquid water content (LWC). Figure 2 displays time series of modeled and observed accumulation of snow water equivalent (SWE). The model produces SWE totals for the Steamboat PHQ location that compare closely to the manually measured PHQ values and nearby automated snow telemetry stations (SNOTEL). The RAMS time series in the figure is from the clean simulation since observations indicate this event to be rather pristine in terms of aerosols.

Figure 3 displays the time series of model and observed cloud LWC (from the FSSP). Both indicate a high LWC orographic cloud event at SPL with values above 0.1 (g kg^{-1}) for much of the time shown. The corresponding cloud droplet number concentrations are shown in figure 4. Here the observed FSSP and the clean and polluted simulations are displayed. The relative agreement between the FSSP and simulated clean event suggests the presence of large cloud droplets and heavy riming, which is what was observed. The polluted simulation provides an idea of the droplet concentrations that could have been supported during such an event if the observed aerosol distribution was similar to the modeled distribution.

The simulated accumulated SWE across the topographic transect shown in figure 1 is displayed in figure 5. The histogram plot reveals the increase in snowfall with elevation as well as the difference that occurs between the clean and polluted model runs. A closer look reveals that as the aerosol concentration increases the SWE totals tend to decrease on the windward slope and increase on the leeward slope. From the background discussion above, we suggest that modification of the orographic cloud by the presence of aerosols tends to modify the seeder-feeder riming process, and thus, the total water content that deposits at the surface. This effect is discussed in more detail in the following sections.

4. IMPACTS OF POLLUTION AEROSOLS

a. CCN Effect

Aerosol particles in the sub-micron range with a dry median radius around 0.04 μm are small enough that high supersaturation is required to overcome curvature effects and become activated. High N_{CCN} leads to high concentrations of small droplets, whereas, low N_{CCN} results in fewer, larger droplets. Smaller droplets have much smaller collection efficiencies, and are less likely to be rimed and contribute to the total surface water. From figure 6, the simulations with the higher N_{CCN} resulted in suppressed snow water equivalent (SWE) on the windward slopes and increased SWE on the leeward slopes. There is not simply a reduction in precipitation everywhere due to the pollution, but rather a re-distribution due to enhanced downstream advection of the more lightly rimed, slower falling crystals in the polluted case. The CCN effect on snowfall exhibits the same trend for different background values of N_{GCCN}, although the increase in N_{CCN} results in a greater modification of snowfall for high N_{GCCN}. GCCN produce larger droplets that have a high riming efficiency. The introduction of a high N_{CCN} counters the GCCN effect by reducing mean droplet size and the degree of riming. Since higher N_{GCCN} lead to more riming and greater snowfall, the addition of CCN have a greater impact when GCCN are numerous.

The modification to the riming process tends to alter the hydrometeor condensate fields. Figure 7 displays the event-averaged west to east cross-section through SPL of hydrometeor mixing ratios for the clean and polluted simulations. First, the addition of pollution aerosols allows for greater LWC in the orographic cloud and a larger area of high LWC. One can also see the increased amount of unrimed or lightly rimed snow and the reduced amount of graupel that is produced as a direct result of reduced riming of cloud droplets due to their smaller size and collection efficiency.

The time series plots of domain summed microphysical quantities in figure 8 help to clarify the competing cloud growth and precipitation processes that vary with aerosol concentrations. For the increase in N_{CCN}, at both low and high N_{GCCN}, the magnitude of riming is diminished, but more so for greater N_{GCCN}. As a result, the amount of existing cloud LWC increases for increasing N_{CCN}, regardless of N_{GCCN}. The curves of cloud nucleation and vapor deposition have opposite trends and are closely inter-related with riming. If N_{CCN} rises, droplets become numerous but smaller; their lifetime in the cloud is longer since they rime less effectively. The persistence of numerous droplets increases the surface area available for vapor growth. As such, the vapor deposition process utilizes excess vapor beyond supersaturation, and the nucleation of new droplets diminishes.

The total domain-summed precipitation change on grid-4, due to an increase in N_{CCN} from 100 to 1900 cm^{-3}, was only 0.7% at low N_{GCCN} and -0.8% at high N_{GCCN}. These domain-wide changes are quite small and exhibit an inconsistent trend in the sign of change.

b. Giant - CCN Effect

The impact of GCCN is nearly opposite to that of CCN. The 3μm radius is large enough that curvature effects offer little inhibition for activation and droplet nucleation. The parcel model results for GCCN suggested that nearly all available GCCN will support

new droplet formation even at modest supersaturation. Furthermore, they nucleate into droplets with considerable initial size, such that riming of these droplets is immediately active. Compared to CCN, further growth by vapor deposition is unnecessary to reach a minimum size prior to riming.

Figure 9 displays the change in SWE precipitation for the given increase in N_{GCCN} at both low and high background values of N_{CCN}. Along the Park Range, this plot depicts nearly a mirror image of the CCN effect. Here the precipitation is increased along the windward slope and decreased along the leeward slope. This is primarily a function of the riming by the seeder-feeder process. Newly formed droplets in the large cloud droplet mode, via GCCN, are readily rimed. While an addition of number concentration would tend to reduce the average droplet size, it is not sufficient to squelch the riming process. Newly formed large droplets offer more sites for riming which leads to increased surface deposition. The introduction of a few large droplets also increases the overall cloud droplet self-collection process and tends to broaden the droplet distribution.

From figure 9, the GCCN effect is greatest in this winter orographic cloud environment at low N_{CCN}. This is contrary to traditional thought for the injection of GCCN in warm rain clouds, but here we are dealing with lower supersaturation, typically smaller droplets, and precipitation modification primarily by riming. Looking at the microphysical time series in figure 8, the amount of riming is maximized at low N_{CCN} and high N_{GCCN}. While the addition of N_{GCCN} in the high N_{CCN} environment helps to stimulate droplet self-collection and riming, perhaps only a limited number of droplets begin to reach the size needed for heavy riming. At low N_{CCN} many of the droplets may already be of riming size. An additional insurgence of GCCN may be enough to trigger the collection needed for growth to optimal riming size. Both the number concentration and size of droplets determine how much riming occurs in-cloud.

The GCCN effect on the seeder-feeder process is to modify the degree of riming. Heavy riming leads to more dense snow crystals and formation of graupel. The model microphysics uses a heat budget computation to determine the amount of rimed water remaining unfrozen. If enough riming occurs to prevent instantaneous freezing, then part of the snow mass distribution is transferred to the graupel category. This category has a greater density and offers less drag, and therefore, it has a greater fall speed. The higher density ice particles deposit further upstream than the low density particles. Figure 10 displays the difference in accumulation of the snow + aggregate SWE and the graupel SWE for the given increase in N_{GCCN}. Over much of the Park Range, the aggregate mass is reduced while the graupel accumulation is enhanced, especially along the windward slope and ridge. The net difference produces a greater concentration of total SWE along the windward slope.

The total domain-summed precipitation change due to an increase in N_{GCCN} from 0.00001 to 0.5 cm^{-3} was 3.2% at low N_{CCN} and 1.6% at high N_{CCN}. The enhancement of GCCN displays an increasing trend in total precipitation, but more so, at lower background N_{CCN} values. Perhaps these larger hygroscopic particles could be used effectively in wintertime weather modification.

4. CONCLUSIONS

In this study, a set of 42 hour simulations were run for a heavy riming and heavy orographic snowfall event beginning 0000 UTC on 11 Feb 2007. RAMS was run for the duration of these cases with varying profiles of maximum CCN and GCCN concentrations. The impact of increasing the CCN concentration leads to a shift in snowfall distribution from the windward slope to the leeward slope due to a reduction in rime growth of ice crystals. An increase in CCN leads to an increase in droplet number but reduction in droplet size. Smaller drops are rimed less effectively, which leads to smaller and less dense ice crystals. The lighter crystals tend to advect further downstream prior to surface deposition. Thus, the blowover effect shifts the snowfall distribution downstream. An increase in GCCN tends to enhance the riming process due to production of large cloud droplets that are readily rimed by snow crystals. Increased riming leads to faster surface deposition, and thus, a shift in snow distribution that favors increased precipitation on the windward slope.

Acknowledgements: This research was supported by the National Science Foundation under grant ATM-0451439 and by UCAR-NCAR-COMET under grant S04-44700.

5. REFERENCES

Borys, R.D. and M.A. Wetzel, 1997: Storm Peak Laboratory: A research, teaching, and service facility for the atmospheric sciences. *Bull. Am. Meteorol. Soc.*, **78**, 2115–2123.

_____, D.H. Lowenthal, and D.L. Mitchell, 2000: The relationships among cloud microphysics, chemistry, and precipitation rate in cold mountain clouds. *Atmos. Environ*., **34**, 2593-2602.

_____, _____, S.A. Cohn, and W.O.J. Brown, 2003: Mountaintop and radar measurements of anthropogenic aerosol effects on snow growth and snowfall rate. *Geo. Res. Lett.*, **30**, 1538, doi:10.1029/2002GL016855.

Hindman, E.E., 1986: Characteristics of supercooled liquid water in clouds at mountaintops in the Colorado Rockies. *J. Clim. Appl. Meteor*., **25**, 1271-1279.

Rauber, R.M., L.O. Grant, D. Feng, and J.B. Snider, 1986: The characteristics and distribution of cloud water over the mountains of northern Colorado during wintertime storms. Part II: Spatial distribution and microphysical characteristics. *J. Climate Appl. Meteor.*, **25**, 489-504.

Saleeby, S.M., and W.R. Cotton, 2004: A large droplet mode and prognostic number concentration of cloud droplets in the Colorado State University Regional Atmospheric Modeling System (RAMS). Part I: Module descriptions and supercell test simulations. *J. Appl. Meteor*., **43**, 182-195.

_____, and _____, 2008: A binned approach to cloud droplet riming implement in a bulk microphysics model. *J. Appl. Meteorl. Climatol*., **47**, 694-703.

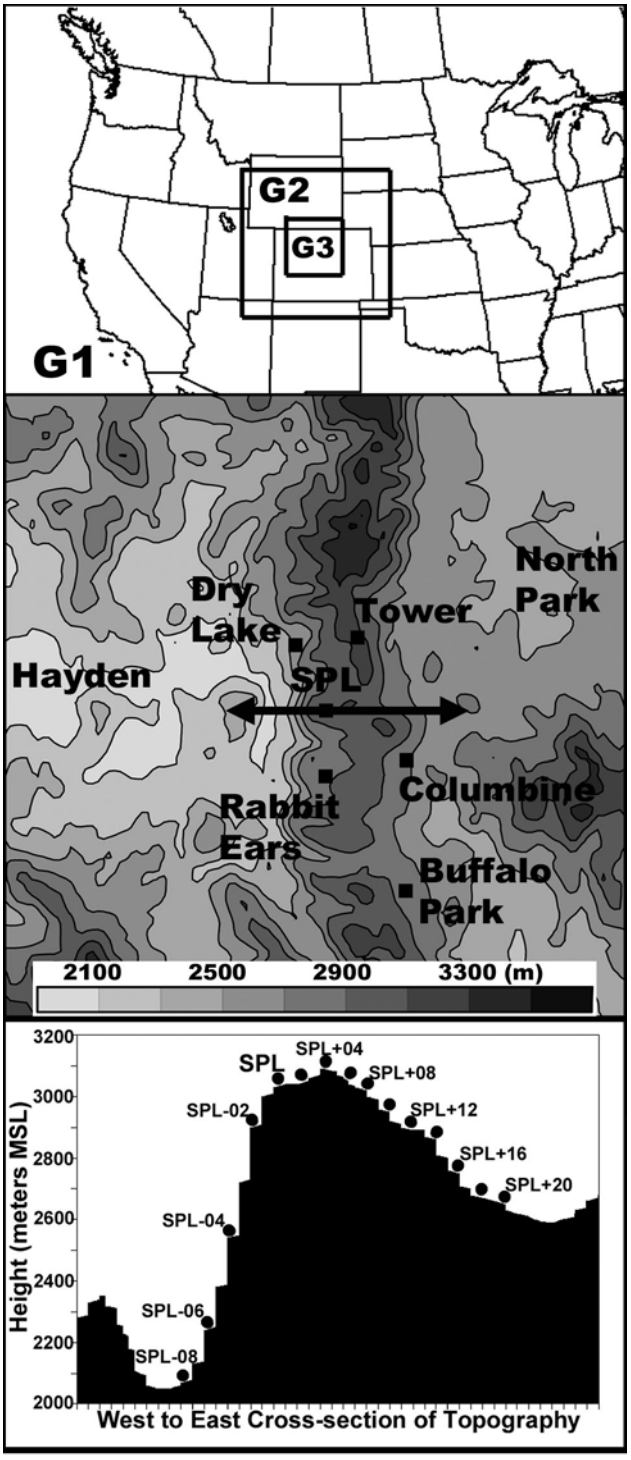

Figure 1. (Top) Model grids. (Middle) The nested Grid-4 over the Park Range with 750m spacing. (Bottom) Model topographic cross-section through SPL and the Park Range as denoted by the arrowed line in the middle panel.

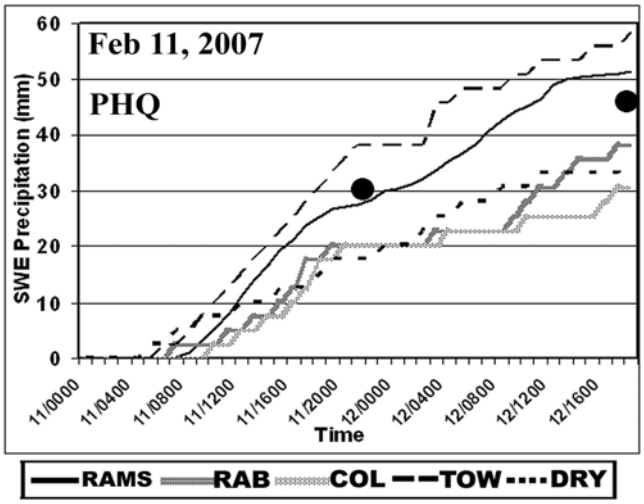

Figure 2. Time series of accumulated SWE from RAMS, several SNOTEL sites (RAB, COL, TOW, DRY), and from manual observations at PHQ (black dots).

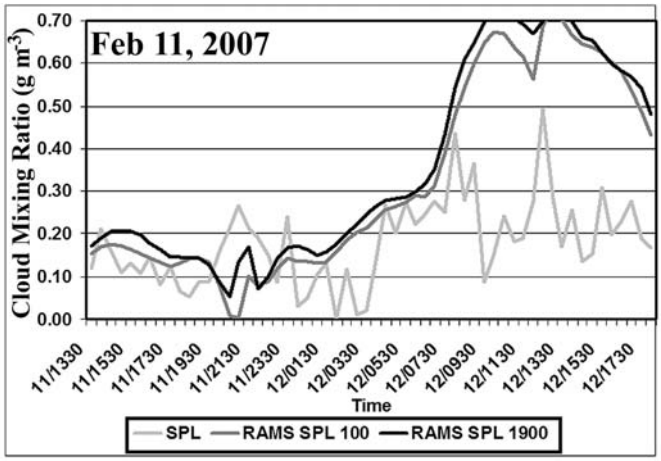

Figure 3. Time series of FSSP observed and RAMS predicted cloud LWC at the location of SPL. The traces are shown for both the clean and polluted simulated events.

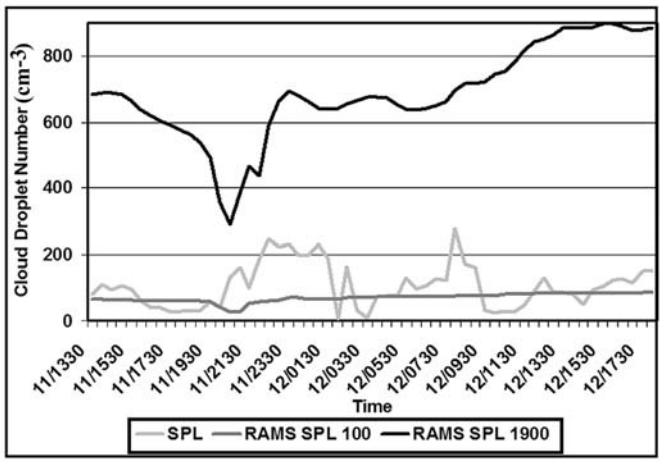

Figure 4. Time series of FSSP observed and RAMS predicted cloud droplet number concentration at the location of SPL. The traces are shown for both the clean and polluted simulated events.

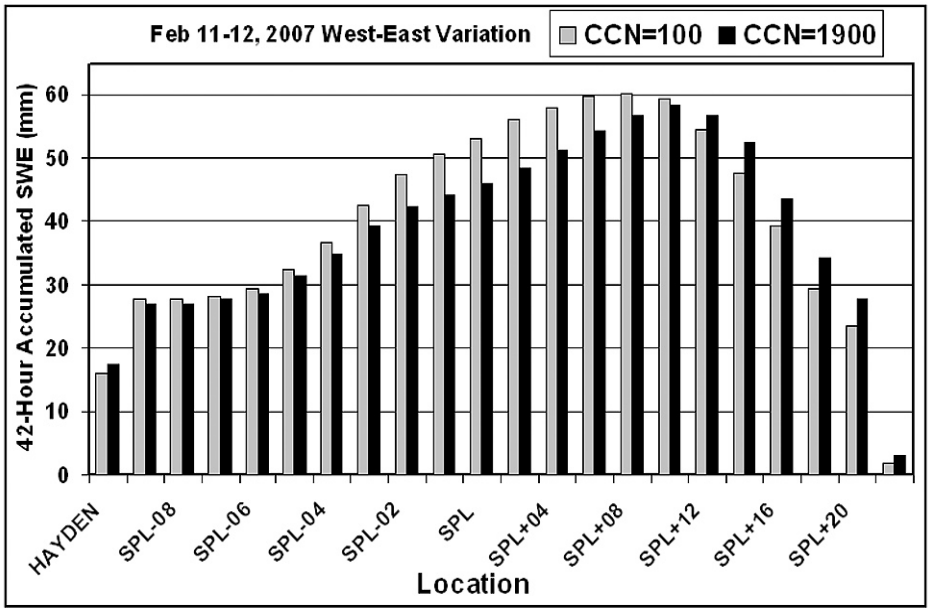

Figure 5. Model accumulated SWE along the Park Range west to east transect through SPL from figures 1. Histogram displays results from both the CCN clean and polluted simulations.

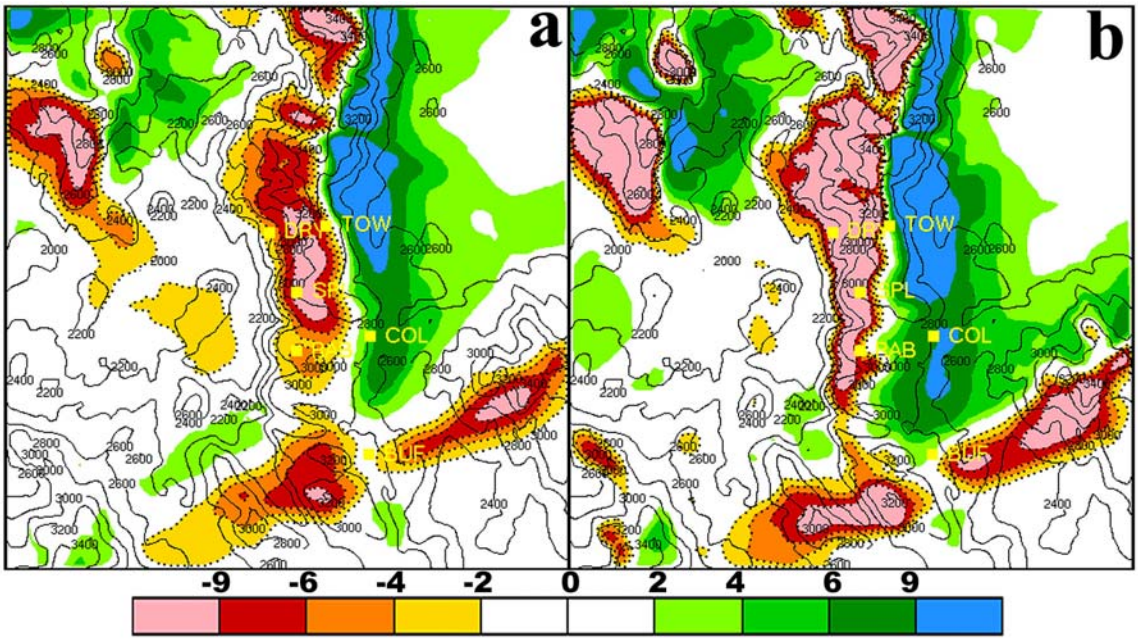

Figure 6. Accumulated SWE difference (mm) for an increase in CCN from 100 to 1900 (cm^{-3}) with GCCN held constant at: (a) 0.00001 and (b) 0.5 (cm^{-3}).

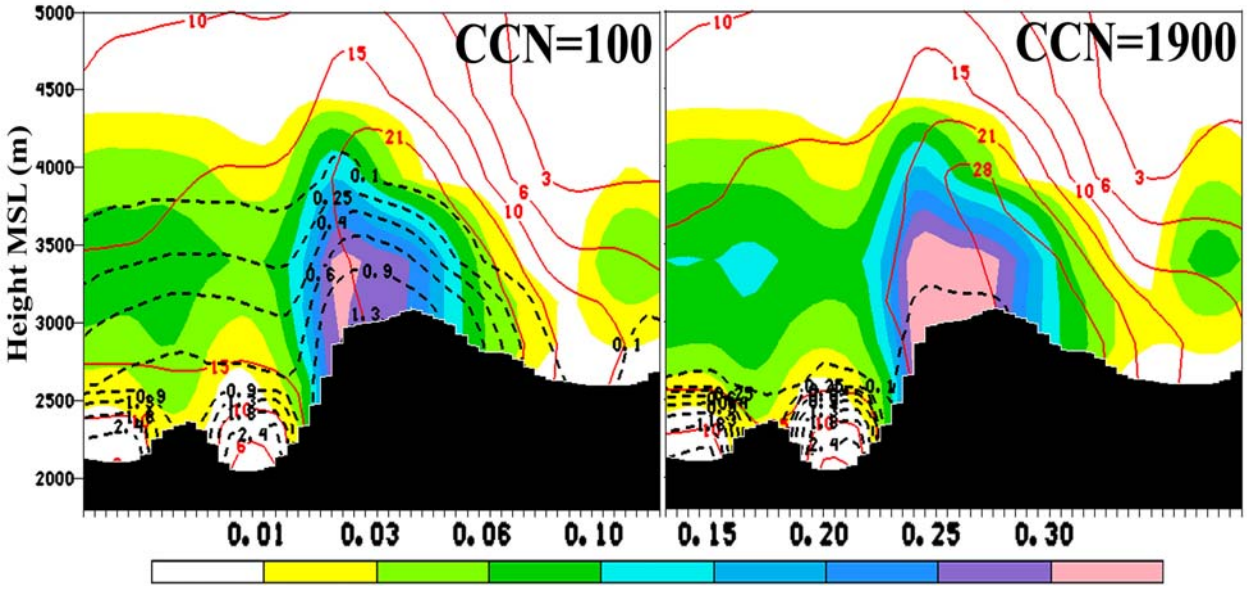

Figure 7. Event averaged mixing ratio of cloud water (g/kg, shaded), snow (g/kg x 100, red solid), and graupel (g/kg x 100, black dashed) for the clean (CCN=100 cm-3) and polluted (CCN=1900 cm-3) events. GCCN were held constant.

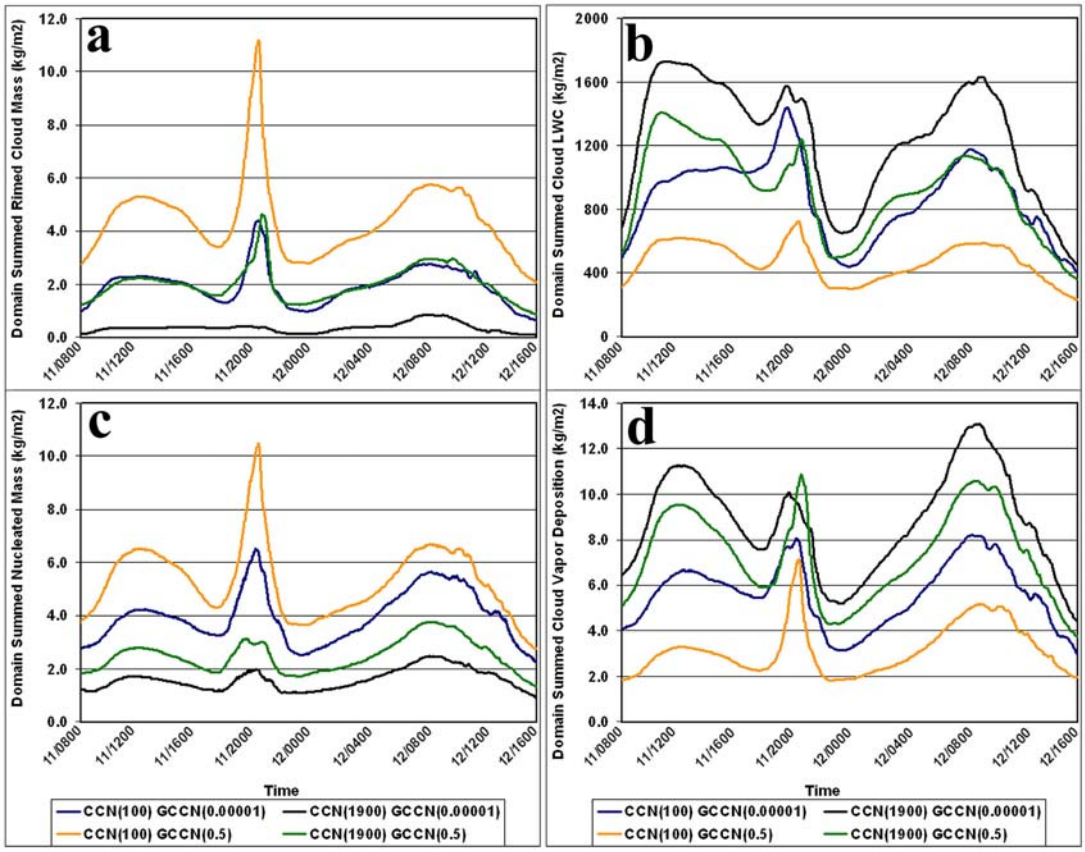

Figure 8. Time series of domain summed mass quantities of (a) rimed cloud water, (b) cloud LWC, (c) nucleated cloud water, and (d) cloud vapor deposition for varying CCN and GCCN concentration. (Curves are identified at the bottom of the plot with the corresponding line color).

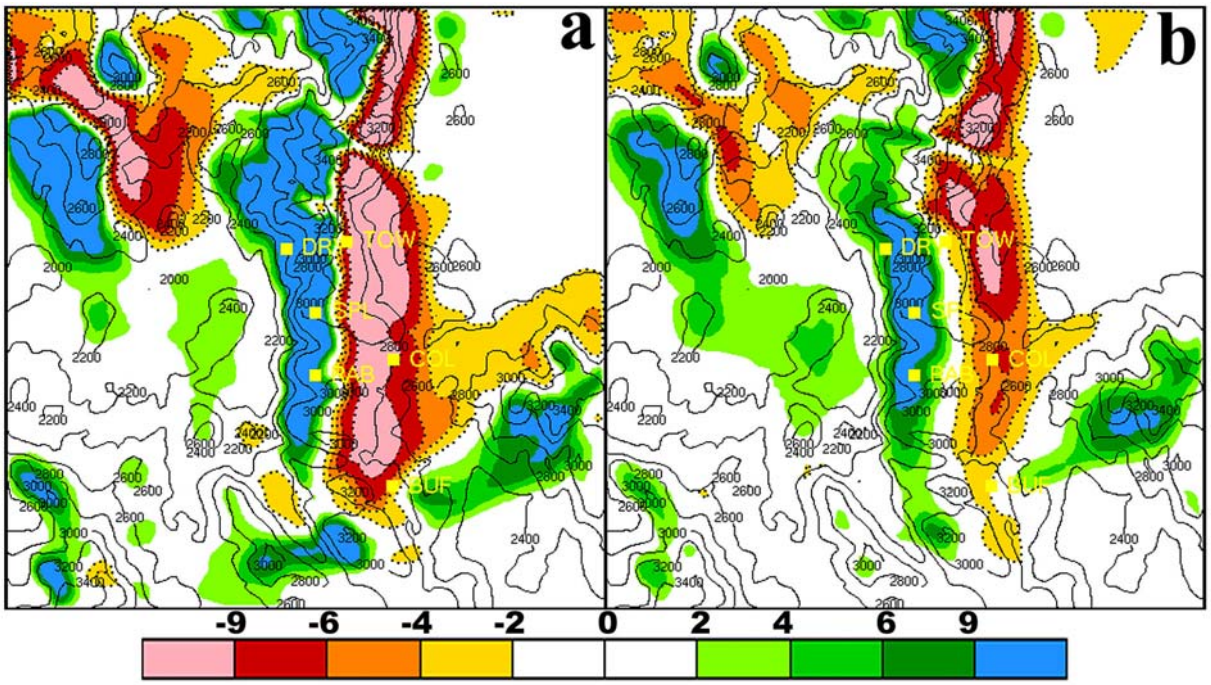

Figure 9. Accumulated SWE difference (mm) for an increase in GCCN from 0.00001 to 0.5 (cm^{-3}) with CCN held constant at: (a) 100 and (b) 1900 (cm^{-3}).

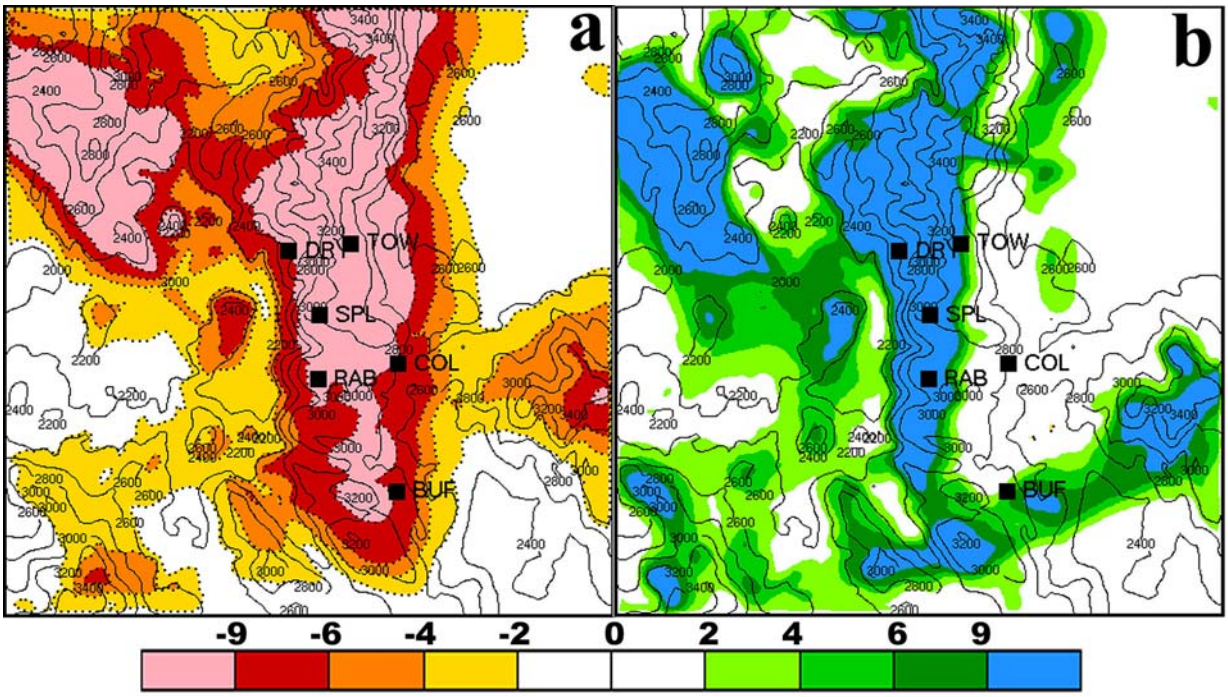

Figure 10. Accumulated difference in SWE (mm) from (a) snow + aggregates and (b) graupel for an increase in GCCN from 0.00001 to 0.5 (cm^{-3}) with CCN held constant at 100 (cm^{-3}).